MODELING OF THE FLOW AROUND A STALLED AIRFOIL USING THE VORTEX METHOD AND THE LAMINAR INTEGRAL BOUNDARY-LAYER THEORY

Marcus V. G.Muniz, marcusmuniz@gmail.com
Victor Santoro Santiago, vsantoro@ig.com.br
Gustavo C. R. Bodstein, gustavo@mecanica.coppe.ufrj.br
Federal University of Rio de Janeiro, Department of Mechanical Engineering – Politécnica/COPPE
Centro de Tecnologia, Bloco G, sala 204 – Ilha do Fundão, 21945-970 Rio de Janeiro, RJ – Brazil

Abstract. *The aerodynamic characteristics of airfoils are extremely important for the design of general lifting surfaces. The incompressible flow around an airfoil depends strongly on the airfoil shape, angle of atack and Reynolds number. When the angle of attack is low, the boundary layer stays attached to the surface of the body, but it separates when the angle of attack is high. At separated conditions (stall), the lifting coefficient drops sharply and the boundary layer vorticity is shed into the flow from the separation points located on the upper surface of the airfoil and at the trailling edge, generating oscillatory aerodynamic loads and wake. In this paper, we use the Discrete Vortex Method coupled with a piecewise-continuous linear-vortex Panel Method distributed over flat panels to simulate the unsteady flow around an aerodynamic profile. For an airfoil subject to stall conditions through a sudden change of the angle of attack, the boundary layer vorticity shedding is modeled employing constant-vorticity panels located at two separation points, one fixed to the trailling edge and the other fixed to the upper surface of the airfoil. The upper surface separation point is predicted applying the method of Walz within the context of the Karman-Pohlhausen integral boundary-layer theory for laminar flows. These separation panels are transformed into Lamb vortices, forming a vortex cloud that moves by diffusion and convection. The induced velocity and the diffusive displacements of the vortices are evaluated by the Biot-Savart law and the Random-Walk Method, respectively. The aerodynamic loads over the airfoil obtained with this model are compared to experimental results available in the literature.*

Keywords*: vortex method, panel method, airfoil, potential flow, boundary-layer separation.*

1. INTRODUCTION

The aerodynamic characteristics of airfoils are important for the design of wings, turbomachine blades, helicopter rotors and other lifting surfaces. Due to the complexity of the physics involved in this problem, elaborate mathematical and numerical models for the simulation of the flow around airfoils have been developed during the past decades. The approach more frequently used nowadays is to solve the Navier-Stokes equations employing sophisticated numerical methods devised to run on a mesh that discretizes the fluid domain and its boundary.

A couple of decades ago, when there were limited computer hardware and incipient numerical methods available, flow modeling was based upon simplifying assumptions, such as irrotational flow. With this approach, it is possible to preserve the main physical flow features and to obtain numerical solutions with low CPU cost and, hopefully, acceptable accuracy for engineering applications (Vezza and Galbraith, 1985). These simplified models are still employed nowadays in preliminary steps of any design process. In this work we adopt this simplified modeling approach to study the incompressible unsteady flow around an airfoil under stall conditions. We use a Lagrangian numerical methodology based upon the Vortex Method (Cottet and Koumoutsakos, 2000) to evaluate the motion of a cloud of Lamb vortices generated near the body surface to model the viscous wake that emanates from the airfoil's separation points. We assume that the boundary layer vorticity is shed into the flow to form the wake from (fixed) calculated separation points. We also assume that the flow is laminar on the entire airfoil surface. The Lamb vortex is the element that transports vorticity through convective and diffusive displacements, evaluated using the Biot-Savart Law and the Random Walk Method (Lewis, 1991), respectively. To compute the potential flow we discretize the airfoil surface with flat panels and use a piecewise-continuous linear-vortex Panel Method (Katz e Plotkin, 2001).

Teixeira *et al*. (2006) present a model for the unsteady incompressible flow around a stalled airfoil based upon the models of Basu and Hancock (1978) and Vezza and Galbraith (1985). Vorticity is shed from fixed separation points at the airfoil upper surface and at the trailing edge. The upper separation point is kept fixed and is input to the code from known experimental data. Constant-vortex panels are used to model the shear layers that emanate from the separation points, which are transformed into Lamb vortices subsequently. The main objective of this paper is to improve one fundamental aspect of the model presented by Teixeira *et al*. (2006): we add a model to evaluate the position of the upper separation point using the Karman-Pohlhausen integral boundary layer theory with the method of Walz (Schlichting and Gersten, 2000), instead of inputting this information from experiments. Ultimately, we wish to develop a simplified, but fast and accurate, model to evaluate the aerodynamic loads over airfoils immersed in a uniform incompressible flow subject to stall.

2. MATHEMATICAL MODEL

Consider a uniform flow around an airfoil that undergoes a sudden change of its angle of attack beyond stall. The boundary layer is laminar, but the Reynolds number is large. At high angle of attack, the boundary layer over the body separates from the trailing edge and from a point on the upper surface of the airfoil, developing shear layers that emanate from these separation points to form the wake downstream of the body. The separation phenomenon at these two points is the only mechanism that sheds vorticity into the wake. We model the shear layers using flat constant-vortex panels that are, eventually, transformed into Lamb vortices. We assume that the flow is two-dimensional, incompressible, unsteady and rotational (in the core of the vortices), governed by the continuity and the Navier-Stokes equations. By taking the curl of the Navier-Stokes equations and using the incompressible continuity equation we obtain the vorticity transport equation, which can be written in nondimensional form for two-dimensional flows as

$$\frac{D\omega}{Dt} \equiv \frac{\partial \omega}{\partial t} + \mathbf{u} \cdot \nabla \omega = \frac{1}{Re} \nabla^2 \omega \, . \tag{1}$$

In Equation (1), $\mathbf{u}$ is the velocity field and ω is the only non-zero component of the vorticity vector, which is normal to the plane of the flow. The Reynolds number is defined as $Re \equiv U_\infty c/\nu$, where U_∞ is the speed of the uniform flow at infinity, c is the airfoil chord and ν is the fluid kinematic viscosity. All the quantities bellow are nondimensionalized by U_∞ e c. As illustrated in Fig. 1, this flow presents two distinct regions: one rotational, region R_2, which incorporates all the wake vorticity and is defined as the region between the two shear layers that emanate from the upper surface and the trailing edge separation points, indicated by a' and b' in Fig. 1; and a second region bounded by points a and b in Fig. 1, region R_1, that is totally irrotational ($\omega = 0$) and corresponds to the flow outside the wake region. In irrotational flow region we can define the velocity potential ϕ, such that $\mathbf{u} \equiv \nabla\phi$, and the Navier-Stokes equation becomes the Euler equation, which produces the unsteady Bernoulli Equation after integration.

2.1. Boundary Layer Modeling

The effect of the boundary layer is taken into account by two models. In the first one, we assume that the boundary layer vorticity is concentrated into a thin vortex sheet distributed over the surface of the body, such that the local jump in the tangential velocity of the sheet is equal to the local sheet strength (Lewis, 1991). In this paper, the vortex sheet strength on the airfoil surface is evaluated using the Panel Method (Katz and Plotkin, 2001) with a piecewise-continuous linear-vortex distribution over flat panels, as shown in Fig. 2.

The second model is intended to estimate the separation point on the upper surface of the airfoil using as initial data the potential flow velocity distribution on the airfoil surface calculated using the panel method. The position of the separation point is evaluated employing the Karman-Pohlhausen integral boundary layer theory coupled with the method of Walz (Schlichting and Gersten, 2000) for laminar flows. According to this methodology, it is assumed that the velocity profiles in the boundary layer correspond locally to a Hartree profile, known as "*local similarity*", which are solutions of the single-parameter Falkner-Skan equation and, therefore, represent a single-parameter profile family based on the Falkner-Skan parameter β. The reader is referred to Schlichting and Gersten (2000) for the details of the theory. The separation point is calculated from the profile parameter $K(s)$, denoted by $\Gamma(s)$ in Schlichting and Gersten (2000), and the thickness parameter Z, which are given by

$$K(s) \equiv -\frac{\delta_2^2}{U}\left(\frac{\partial^2 u}{\partial y^2}\right)_w = \frac{Z}{U}\frac{dU}{ds}\,, \tag{2a}$$

$$Z(s) \equiv \frac{\delta_2^2 U}{Re} = \frac{a}{\left[U(s)\right]^b}\int_0^s U^b(\xi)\mathrm{d}\xi \,, \tag{2b}$$

where s is a local tangential coordinate along the airfoil surface with origin located at the trailing-edge and going around the airfoil in the counterclockwise direction, $\delta_2(s)$ is the momentum thickness, $U(s)$ is the potential flow velocity on the airfoil surface and $(\partial^2 u/\partial y^2)_w$ is the concavity of the boundary layer velocity profile at the wall. If x is the coordinate coinciding with the chord line with origin at the leading-edge, then $s = s(x)$, and the separation point x_s is the position along the airfoil chord where the profile parameter K takes the value $K(x_s) = K_s$. For the method of Walz, the parameter K is in the range $-0.10 < K < 0.10$ and is calculated with $a = 0.441$ and $b = 4.165$, if $K > 0$, and $a = 0.441$ and $b = 4.579$, if $K < 0$. Separation occurs when $K_s = -0.0681$.

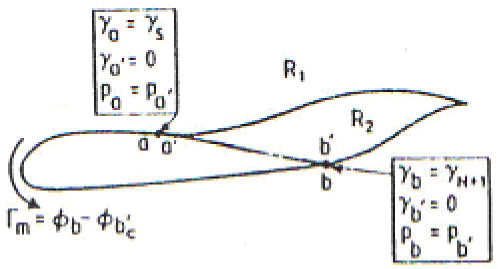

Figure 1. Airfoil with fixed separation points: regions R_1 and R_2 of the flow (Vezza and Galbraith 1985).

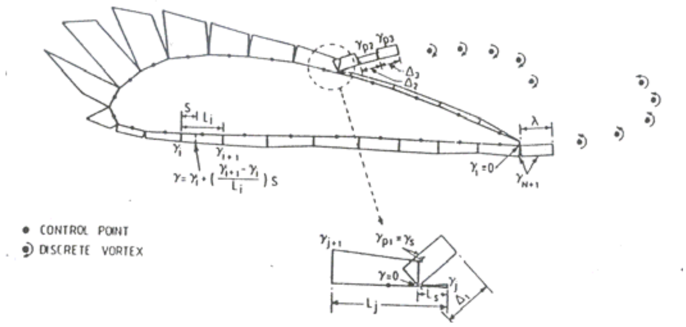

Figure 2. Airfoil with the panels, separation points and additional unknowns due to extra panels (Vezza and Galbraith, 1985).

2.2. Unsteady Kutta Condition

In order to obtain a unique solution, it is necessary to impose the Kutta condition, which expresses a condition of continuity of the static pressure at the separation points of the airfoil and is related to the vorticity shedding at these points. The unsteady Kutta condition can be described as a function of the circulation Γ around the airfoil and the strength of the constant-vortex panels at the upper separation point, γ_s, and at the trailing edge, γ_{N+1} (shown in Figs. 1 and 2) according to the equation

$$\frac{\gamma_s^2}{2} - \frac{\gamma_{N+1}^2}{2} = \frac{\partial \Gamma_m}{\partial t} \cong \frac{\Delta \Gamma_m}{\Delta t} . \tag{3}$$

2.3. Vortex Convection and Diffusion

In the rotational region of the wake, where the flow is governed by the vorticity transport equation – Eq. (1), all the vorticity is modeled as a cloud of Lamb vortices. To capture the solution of Eq. (1), each vortex in a cloud of N_v vortices must convect according to the following system of ordinary differential equations

$$\frac{d\mathbf{x}_i}{dt} = \begin{bmatrix} 0 & -1 \\ 1 & 0 \end{bmatrix} \sum_{j=1}^{N_v} \frac{\Gamma_j}{2\pi} \frac{\mathbf{x}_i - \mathbf{x}_j}{\left|\mathbf{x}_i - \mathbf{x}_j\right|^2} \left[1 - \exp\left(-\frac{\left|\mathbf{x}_i - \mathbf{x}_j\right|^2}{4\sigma_i^2} \right) \right], \tag{4}$$

where vortex i has strength Γ_i, position $\mathbf{x}_i$ and core radius $\sigma_i \equiv (\nu t)^{1/2}$, for $1 \le i \le N_v$. The velocity on the right-hand side of Eq. (4) comes from integration of the Biot-Savart law to compute the induced velocities of the vortices.

2.4. Pressure Distribution Over the Airfoil Surface

The pressure distribution is obtained from the Euler equation calculated on the airfoil surface, which can be written in nondimensional form as

$$\frac{\partial p_0}{\partial s} = -\frac{\partial U}{\partial t}, \tag{5}$$

where s again is the coordinate along the surface, p_0 is the stagnation pressure defined as $p_0 \equiv p + U^2$, p is static pressure, U is the potential flow velocity on the body surface in the s direction, and t is time. The static and stagnation pressures are nondimensionalized by $\rho U_\infty/2$, where ρ is the fluid density.

3. NUMERICAL METHOD

The contribution of the airfoil to the entire flow is obtained using a piecewise-continuous linear-vortex Panel Method (Katz e Plotkin, 2001). We model the vorticity of the shear layer that emanates from the separation points fixed at the upper surface and at the trailing edge with constant-vortex panels and the vorticity present in the wake with Lamb vortices. The Discrete Vortex Method is responsible for the evaluation of the vorticity transport in the flow.

3.1. Panel Method

The panel method (Katz e Plotkin, 2001) is employed to evaluate the potential flow. As illustrated in Fig. 2, the body contour is discretized into small flat or curved elements, called panels, which possess a distribution of mathematical singularities, such as source, doublet or vortex, along their length. We use flat panels with a vorticity distribution that varies linearly along the panel length. The panel middle point, called control (or collocation) point, is the location where the impermeability condition is imposed, whereas the panel endpoints, called nodes (or nodal points), are the boundary points where the unknown strength γ_i of the linear-vortex distribution of the panels are calculated.

3.2. System of Linear Algebraic Equations

The discretization of the body into N panels with linear vorticity distribution subject to the impermeability boundary condition imposed at the N collocation points of the airfoil panels leads to N linear algebraic equations. The unknowns are the N+1 node values of γ_i, that is, γ_1 to $\gamma_{N+1,}$ the two unknowns related to the strength of the extra panels with constant vorticity that model the vorticity shedding at the separation points, one at the trailing edge and the other at the upper surface of the airfoil, γ_w and γ_s, and the two unknowns related to the strength on either side of the extra panel located at the upper surface separation point of the airfoil, γ_s^+ and γ_s^-. Therefore the system contains N equations and N+5 unknowns. Figure 2 helps to define these quantities. Following the model of Vezza and Galbraith (1985), we assume: $\gamma_s^+ = 0$, $\gamma_1 = 0$, $\gamma_s^- = \gamma_s$ and $\gamma_{N+1} = \gamma_w$, where γ_w is the strength of the constant-vortex extra panel at the trailing edge. Hence, the linear system of algebraic equations that represents the impermeability condition on the i^{th} panel of the airfoil for the incompressible two-dimensional unsteady flow studied in this paper present the same standard configuration that characterizes the steady-flow linear-vortex panel method, with N equations and N+1 unknowns (Katz e Plotkin, 2001). This system of equations may be concisely written as

$$\mathbf{U}_\infty \cdot \mathbf{n}_i + \sum_{j=1}^{N+1} A_{ij}\gamma_j + A_{is}\gamma_s + A_{iw}\gamma_w + \sum_{k=1}^{N_e} A_{ik}\gamma_k + \sum_{n=1}^{N_v} G_{in}k_n = 0 \,. \tag{6}$$

The coefficients in Eq. (6) and their mathematical derivations can be found in Teixeira (2006). This system still requires the unsteady Kutta condition for the solution to be unique. If where Γ_{m-1} and Γ_m are the airfoil circulation at t_{m-1} and t_m, and Δ_1 and λ are the lengths of the upper separation and the trailing edge panels, respectively, Eq. (2) can be expanded (Teixeira, 2006) in the form

$$\Delta_1\gamma_s + \lambda\gamma_{N+1} = \Gamma_{m-1} - \Gamma_m \,, \quad \text{with} \quad \Delta_1 \equiv -\gamma_s\Delta t/2 = \left|\gamma_s\Delta t/2\right| \quad \text{and} \quad \lambda \equiv \gamma_1\Delta t/2 = \left|\gamma_{N+1}\Delta t/2\right| . \tag{7a,b,c}$$

The system formed by Eqs. (6) and (7a) is solved each time step with the aid of Eqs. (7b,c), generating N_e extra panels at the upper surface of the airfoil with known strength and length at the N_e initial time steps. Two Lamb vortices are created at the subsequent time step, with strength given by the product of the strength by the length of the last extra panel. These vortices generate the viscous wake, which will make the flow evolve from a step-function initial condition to a statistically-permanent oscillatory flow. The points from which these two nascent vortices are created correspond to a distance $\gamma_{N+1}\Delta t$ and $\gamma_{Ne}\Delta t$ from the collocation points of the panels at the trailing edge and the last extra panel, in the direction of the panels. The lengths of the separation extra panels λ and Δ_1 are obtained iteratively, solving the equations formed by Eqs (6), and (7) successively for each time step until a converged valued is reached. The initial value of the iteration is taken to be the average length of the airfoil panels and, at subsequent time steps, the initial values are taken to be the converged values from the previous time step. At the initial time of the simulation, when the flow is irrotational, the system of equations is formed by Eq. (6), containing only the first two terms (that correspond to the uniform flow and the airfoil panels) and the Kutta condition for steady flow, expressed as $\gamma_1 + \gamma_{N+1} = 0$ for flat panels with linear vorticity distribution. The solution to the linear system of algebraic equations (6) supply the tangential velocity at the airfoil surface $U(s) = \gamma(s)$ (and its derivative $\mathrm{d}U/\mathrm{d}s$) to evaluate Z and K in Eqs. (2), where $\gamma(s)$ is evaluated at the control point located at the position s as the arithmetic mean of the values of γ at the panel nodes.

The angle β_{sep} between the separation extra panel and the corresponding separation panel at the upper surface of the airfoil and the angle $\Delta\beta_{\text{sep}}$ between adjacent pairs of extra panels are both input data and are kept constant during the simulation. These angles are based either upon mean experimental data for separated flows over airfoils (Vezza and Galbraith, 1985) or numerical experiments run with our numerical model. On the other hand, the angle between the trailing-edge panel and the airfoil chord line, which is obtained by iteration in Vezza and Galbraith (1985), is modeled here according to Mook and Dong (1994), following the model of Teixeira *et al.* (2006). As shown in Fig. 3, the vorticity is shed from the trailing edge as a constant-vortex extra panel in a direction tangent to the lower surface of the body when the circulation around the airfoil increases in time, and in a direction tangent to the upper surface when the circulation decreases in time.

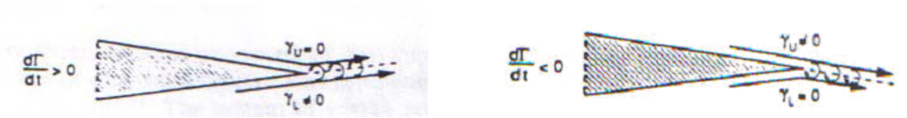

Figure 3. Physical Model to the flow at the trailing edge (Mook and Dong, 1994).

3.3. Evaluation of the Separation Point

As described in section 2.1, the separation point x_s occurs when $K(x_s) \equiv K_s = -0.0681$, for K and Γ calculated from Eqs. (2). Using a linear distribution for $U(s)$ and forward finite differences for dU/ds, Eqs. (2) can be written in descretized form as

$$Z_{i+1} \equiv \left(\frac{U_i}{U_{i+1}}\right)^b Z_i + \left(\frac{a}{1+b}\right) \frac{\left[1-\left(\frac{U_i}{U_{i+1}}\right)^{b+1}\right]}{1-\left(\frac{U_i}{U_{i+1}}\right)} \left(x_{i+1} - x_i\right), \tag{8a}$$

$$K_{i+1} \equiv \left(\frac{Z_{i+1}}{U_{i+1}}\right) \frac{\left(U_{i+1} - U_i\right)}{\left(x_{i+1} - x_i\right)}. \tag{8b}$$

At the first step of the simulation, x_s is evaluated from the potential flow around the airfoil subject to a zero angle of attack. From the second step on, the angle of attack is changed to the value of the simulation, maintaining the separation point evaluated at the first time step and using $U(s)$ from the potential flow solution. The simulation evolves up to $t = 6$, with time-integrated values of $\gamma = U(s)$ being computed in the range $t = 3$ to $t = 6$, when a new separation point is evaluated employing these mean values of γ for the panels. The separation panels are, then, moved to the new value of x_s and the simulation evolves from $t = 6$ to $t = 12$, with another new value of x_s being calculated with mean values of γ computed in the range $t = 9$ to $t = 12$, and so on. This procedure is repeated for every period of 6 units of (nondimensional) time, until $t = 24$ is reached. Our numerical experiments show that this total simulation time is enough for the flow to reach a staticaslly-permanent oscillatory regime and for the value of x_s to converge.

3.4. Discrete Vortex Method

In the Discrete Vortex Method the dynamics of the vorticity shed into the wake from the separation points is simulated with a cloud of Lamb vortices that convect and diffuse vorticity as they move in the flow as Lagragian particles. The temporal evolution of the flow is governed by Eq. (1), decomposed into one purely convective and diffusive vorticity equations (Chorin, 1973), written in the form

$$\frac{\partial \omega}{\partial t} + \mathbf{u} \cdot \nabla \omega = 0 \quad \text{and} \quad \frac{\partial \omega}{\partial t} = \frac{1}{Re} \nabla^2 \omega. \tag{9a,b}$$

To evaluate the velocity $\mathbf{u}$ of a specific vortex it is necessary to add the velocity contributions due the uniform flow, the body panels, the constant separation panels and the vortex cloud. The convective displacement of the vortices, $\Delta \mathbf{x}_c$, is evaluated by integration of Eq. (4) with the 2nd-order Adams-Basthford time-marching scheme, *i.e.*,

$$\Delta \mathbf{x}_c = \left(\frac{3}{2}\mathbf{u}_m - \frac{1}{2}\mathbf{u}_{m\text{-}1}\right)\Delta t. \tag{10}$$

The diffusive process is simulated with the aid of the Random Walk Method (Lewis, 1991), where two random numbers P and Q, drawn from a uniform probability distribution, are used to calculate the random Cartesian displacement of the vortices in the x and y direction, respectively, given by

$$\zeta = \sqrt{\frac{8\Delta t}{Re} \ln\left(\frac{1}{P}\right)} \cos(2\pi Q) \quad \text{and} \quad \eta = \sqrt{\frac{8\Delta t}{Re} \ln\left(\frac{1}{P}\right)} \,\mathrm{sen}(2\pi Q). \tag{11a,b}$$

The total displacement is given by the sum of diffusive and convective displacements, *i.e.*,

$$x(t+\Delta t) = x(t) + \Delta x_c + \zeta \quad \text{e} \quad y(t+\Delta t) = y(t) + \Delta y_c + \eta. \tag{12a,b}$$

3.5. Evaluation of the Pressure Coefficient

The methodology used in this work to evaluate the static pressure, p, on the surface of the airfoil is inspired on the method of Lewis (1991), which does not require the knowledge of the velocity potential, ϕ, as in Vezza and Galbraith (1985). Integrating Eq. (5) for the two regions R_1 and R_2 defined in Fig. 1, the expression for p at the collocation point m of each region is obtained. Thus, using an index m to specify the collocation points and the value m = IPANEL for the collocation point of the upper separation panel, the nondimensional static pressures are given by

$$R_1:\quad p_m = -\sum_{n=1}^{m} 2[\gamma_n(t+\Delta t) - \gamma_n(t)]\Delta s_n / \Delta t - \gamma_m^2\,, \qquad \text{for } 1 \le m \le \text{IPANEL}\,, \tag{13a}$$

$$R_2:\quad p_m = p_{m-1} - 2[\gamma_m(t+\Delta t) - \gamma_m(t)]\Delta s_m / \Delta t + \gamma_{m-1}^2 - (\gamma_m^2 + \gamma_s^2)\,, \qquad \text{for } m = \text{IPANEL}+1\,, \tag{13b}$$

$$p_m = p_{m-1} - 2[\gamma_m(t+\Delta t) - \gamma_m(t)]\Delta s_m / \Delta t + \gamma_{m-1}^2 - \gamma_m^2\,, \qquad \text{for IPANEL}+2 \le m \le M\,, \tag{13c}$$

where γ_m and γ_n are the vorticity at the panel collocation points and γ_s represents the jump in the stagnation pressure as the separation point is crossed from R_1 to R_2. Knowing the pressure at the collocation points from Eqs. (13) and the stagnation pressure (maximum p_m), the pressure coefficients can be evaluated using the expression $C_p(m) = p_m + 1 - p_0$. The aerodynamic loads can be determined by integrating $C_p(m)$ on the body surface.

4. RESULTS AND DISCUSSION

In this section we present results of our simulations of the flow around the GU25-5(11)8 airfoil section. This airfoil belongs to a family of sections that have been developed for man-powered flight (Cotton and Galbraith, 1989). We have chosen this airfoil in order to compare our numerical results with the experimental data obtained by Kelling (1968) and presented in graphic form in Cotton and Galbraith (1989) for a (laminar) Reynolds number of Re = 70,000 and angle of attack $\alpha = 12.6°$. In all simulations the values of the following numerical parameters have been kept fixed: number of panels, N = 46; angle between the separation extra panel and the corresponding separation panel at the upper surface of the airfoil, $\beta_{\text{sep}} = 10°$; angle between adjacent pairs of extra panels, $\Delta\beta_{\text{sep}} = 0°$; radius of the Lamb vortex core, $\sigma = 0.05$; final time of the simulation, t = 24. The values of the number of extra panels, N_e, the time step, Δt, and the number of time steps, M, depend on the simulation. We have run four cases, according to the value of the time step and the number of extra panels: $\Delta t = 0.04$ and $N_e = 5$; $\Delta t = 0.02$ and $N_e = 10$; $\Delta t = 0.01$ and $N_e = 20$; $\Delta t = 0.005$ and $N_e = 40$. Note that these pairs of values for Δt and N_e are chosen such that the length of the shear layer that emanates from the upper separation point is approximately 0.2. With this choice, we believe that the physics is well represented for this type of simulation.

Figure 4 presents the convergence of the upper separation point during the evolution of the simulation and the variation of the converged values as the time step is reduced. Figure 4(a) shows the convergence of x_s as a function of time for all four values of Δt. The results for $\Delta t = 0.005$, $\Delta t = 0.01$ and $\Delta t = 0.02$ coincide with each other and the value of x_s converges to 0.275 from t = 12 on. The converged x_s for the coarsest value $\Delta t = 0.04$ is $x_s = 0.225$, as shown in Figure 4(b), which is not as close to the experimental results, as discussed in the C_p analysis below.

In order to provide a visualization of the early stages of the wake evolution, Figure 5 shows the position of the wake vortices at t = 6 (end of the first cycle). Figures 5(a) and 5(b) correspond to the cases run with $\Delta t = 0.01$ and $\Delta t = 0.005$, respectively, since they are the most accurate. Both wakes illustrate the boundary-layer separation process occurring at x_s and at the trailing-edge and the associated oscillatory vortex shedding and roll-up mechanisms that form counter-rotating vortex pairs. As expected, the case run with $\Delta t = 0.005$ presents finer resolution.

Figure 6 depicts the oscillatory time history of the lift and drag coefficients. We observe an approximate periodic behavior within the period t = 12–24, which is used to calculate time-integrated averages for C_p and C_l. This procedure is carried out over the last 3 time units of each of the two periods of 6 time units that we use to estimate x_s, as described in section 3.3. The arithmetic mean of these two time-integrated averages provide the following values for the lift coefficients: $C_l = 0.82$, computed for $\Delta t = 0.01$; and $C_l = 0.78$, for $\Delta t = 0.005$. As a reference, the experimental value is $C_{l,\text{exp}} = 0.74$. Our computed results are about 10% and 5%, respectively, higher than the experimental one. We should point out that this experimental value is only approximate, since it has been read off the graph (Figure 13) of Cotton and Galbraith (1989) (in addition to the experimental uncertainties of the experiment itself).

Figure 7 shows the mean pressure coefficient distribution over the airfoil chord for $\Delta t = 0.01$ and $\Delta t = 0.005$. Both C_p distributions are very similar, indicating that the position of the separation point is well estimated with the method of Walz. On the upper airfoil surface, the general shape of each graph shows a slightly overpredicted suction peak at x = 0.10, approximately, a separation plateau covering the region $0.275 < x < 0.70$, and a secondary suction peak in the trailing-edge region, due to a high concentration of wake vortices in that area. As pointed out by Teixeira *et al.* (2006), the parameters associated with the extra panels, N_e, β_{sep} and $\Delta\beta_{\text{sep}}$, have a non-negligible effect on the simulation. In addition, the number of panels that we use, N = 46, produces a fairly coarse mesh on the airfoil surface. All these combined effects are responsible for the discrepancies in C_p and C_l.

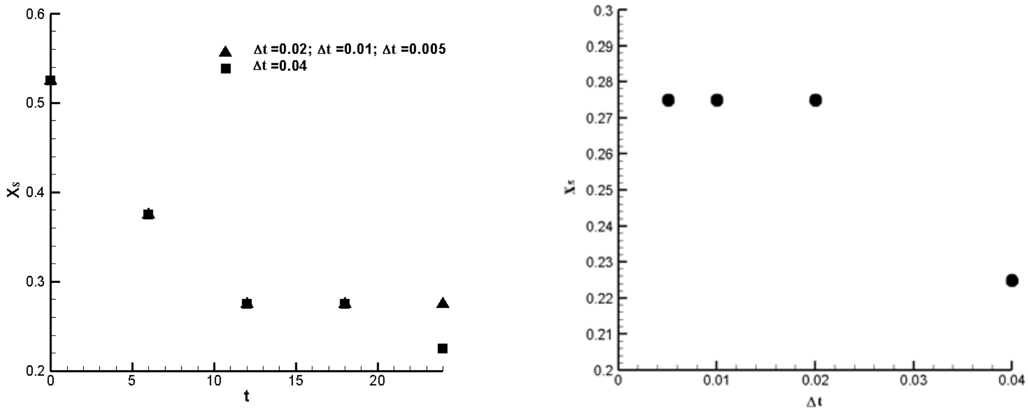

(a) effect of t; (b) effect of Δt

Figure 4. Convergence of the separation point as a function of t and Δt.

(a) $\Delta t = 0.01$; (b) $\Delta t = 0.005$;

Figure 5. Position of the wake vortices at $t = 6$ for $\Delta t = 0.01$ and $\Delta t = 0.005$.

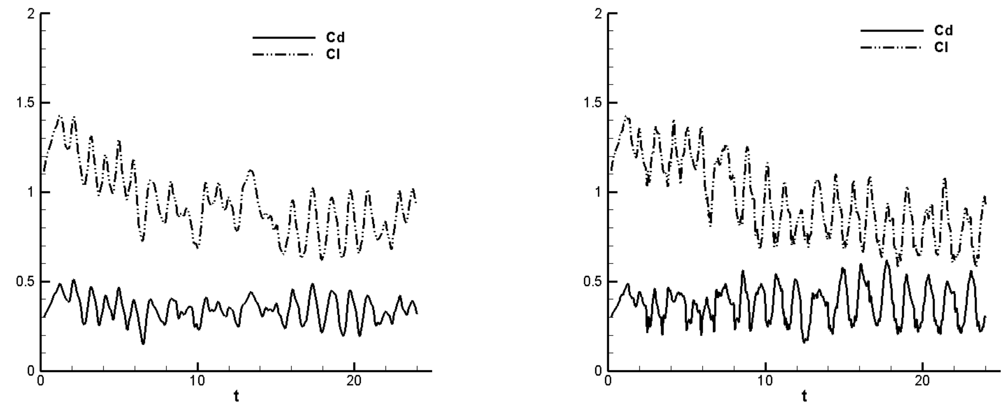

(a) $\Delta t = 0.01$; (b) $\Delta t = 0.005$;

Figure 6. Time history of the drag and lift coefficients for $\Delta t = 0.01$ and $\Delta t = 0.005$.

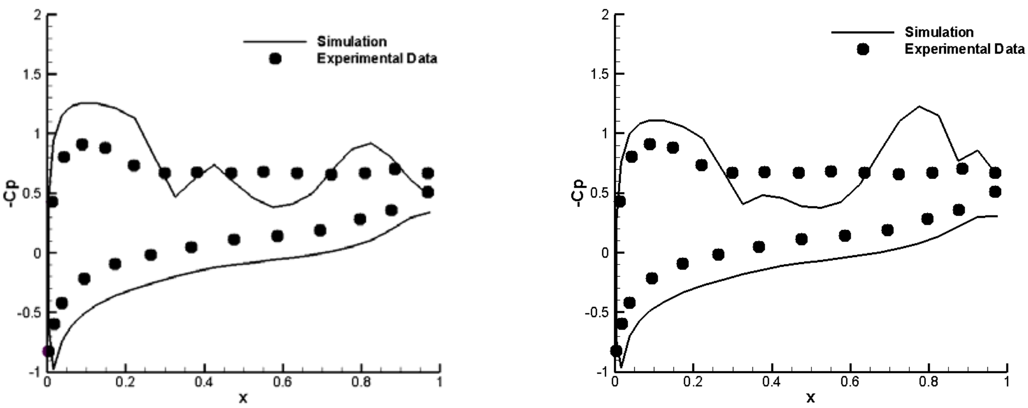

(a) $\Delta t = 0.01$; (b) $\Delta t = 0.005$;

Figure 7. Pressure coefficient distribution along the chord for $\Delta t = 0.01$ and $\Delta t = 0.005$.

5. CONCLUSIONS

We have modeled the two-dimensional unsteady incompressible flow around a stalled airfoil using the Discrete Vortex Method coupled with a linear-vortex panel method and the integral boundary-layer theory to calculate the separation point. Our numerical simulations indicate that the runs for $\Delta t = 0.01$ and $\Delta t = 0.005$ furnish results similar to experimental data, both in terms of accuracy and general physical behavior. Although the run for $\Delta t = 0.02$ converges for the same separation point, the results are considered not as accurate as the other two cases. In particular, because the accuracy of the simulation is related to the convective stepping of the vortices, we note that the value $\Delta t = 0.01$ for the time step corresponds to a quarter of the panel size, approximately. As these results attest, this stepping procedure is enough to guarantee reasonable accuracy and quick runs for this type of simulation, and there is no need to use tighter values of the time step, such as $\Delta t = 0.005$ in this case. Therefore, we believe that if Δt is approximately $\Delta s/4$, where Δs is the average panel size, the simulation will provide reasonably good results for the early stages of design applications. However, there is still need to further investigate the influence of the numerical parameters associated with the separation extra panel and, if possible, to model them, in such a way that these numerical parameters are all calculated during the simulation instead of being input to the numerical code.

6. ACKNOWLEDGEMENTS

The authors would like to acknowledge the financial support to this research project provided by CNPq and the Brazilian Army.

7. REFERENCES

Basu, B.C. and Hancock, G.J., 1978, “The Unsteady Motion of a Two-Dimensional Airfoil in Incompressible Inviscid Flow”, Journal of Fluid Mechanics, Vol. 87, No. 1, pp. 157-78.

Chorin, A.J., 1973, “Numerical Study of Slightly Viscous Flows”, Jounal of Fluid Mechanics, Vol. 57, pp. 785-796.

Cotton, F. N. and Galbraith, R.A.McD., 1989, “A Direct Viscid-Inviscid Interaction Scheme for the Prediction of Two-Dimensional Airfoil Lift and Pitching Moment in Incompressible Flow”, Aeronautical Journal, Vol 93, April, pp. 132-140.

Cottet, G.H. and Koumoutsakos, P.D., 2000, “Vortex Methods: Theory and Practice”, Cambridge University Press, Cambridge, UK.

Katz, J. and Plotkin, A., 2001, “Low - Speed Aerodynamics”, 2nd edition, Cambridge University Press.

Kelling, F. H., 1968, “Experimental Investigation of a High-Lift Low-Drag Airfoil”, Glasgow University Report No. 6802.

Lewis, R.I., 1991, “Vortex Element Methods for Fluid Dynamic Analysis of Engineering Systems”, Cambridge, Cambridge University Press.

Mook, D.T. and Dong, B., 1994, “Perspective: Numerical Simulations of Wakes and Blade-Vortex Interaction”, Journal of Fluids Engineering, Vol. 116, pp. 6-21.

Schlichting, H., and Gersten, K., “Boundary Layer Theory”, Springer, 8th Edition, 2000.

Teixeira, I.R., 2006, “Simulação Numérica do Escoamento Potencial Não-Permanente ao Redor de um Aerofólio com Ponto de Separação Fixo”, Projeto Final de Curso de Graduação, Departamento de Engenharia Mecânica – Poli/UFRJ.

Teixeira, I. R., Santiago, V. S., Bodstein, G. C. R., 2006, “Modelagem Numérica do Escoamento Incompressível Não-Permanente ao Redor de um Aerofólio com Ponto de Separação Fixo”, Paper 17-545, Anais do IV Congresso Nacional de Engenharia Mecânica - CONEM, 22 a 25 de Agosto 2006, Recife, PE, pp. 1-10.

Vezza, M., and Galbraith, R.A.McD., 1985, “An Inviscid Model of Unsteady Airfoil Flow with Fixed Upper Surface Separation”, International Journal for Numerical Methods in Fluids, Vol 5, pp. 577-592.

8. RESPONSIBILITY NOTICE

The authors are the only responsible for the printed material included in this paper.